



Dynamic Analysis of a Microgripper and Its Components

M. Tecpoyotl-Torres^{1*}, P. Vargas-Chable², S. Robles-Casolco¹
and R. Cabello-Ruiz²

¹Centro de Investigación en Ingeniería y Ciencias Aplicadas, CIICAp- Universidad Autónoma del Estado de Morelos, Mexico.

²Doctorado en Ingeniería y Ciencias Aplicadas, CIICAp- Universidad Autónoma del Estado de Morelos, Mexico.

Authors' contributions

This work was carried out in collaboration between all authors. Author MTT designed the study, author PVC performed the statistical analysis, wrote the protocol, and wrote the first draft of the manuscript and managed literature searches. Authors SRC and RCR managed the analyses of the study and literature searches. All authors read and approved the final manuscript.

Article Information

DOI: 10.9734/BJAST/2015/18042

Editor(s):

(1) Osiris Wanis Guirguis Saleh, Biophysics Department, Cairo University, Egypt.

Reviewers:

(1) Shouetsu Itou, Department of Mechanical Engineering, Kanagawa University, Japan.

(2) Anonymous, University of Missouri-St. Louis, USA.

(3) Subramaniam Jahanadan, Physics Unit, Kolej Matrikulasi Labuan, Malaysia.

Complete Peer review History: <http://www.sciencedomain.org/review-history.php?id=1139&id=5&aid=9424>

Original Research Article

Received 31st March 2015
Accepted 9th May 2015
Published 26th May 2015

ABSTRACT

This paper is focused on the dynamic analysis and simulation of a novel microgripper and its components: microcantilever and V-shape thermal actuator. These devices are designed on silicon and implemented on Professional Autodesk Inventor 2014. Simulations were realized using Ansys Workbench Software.

This analysis is common for cantilever, and RF MEM devices, but it is has not been widely realized for other structures, such V-actuator and microgrippers.

The analytical response was acquired with Steady-State Thermal, Static Structural, Modal and Harmonic Response modules.

The dynamic behavior, resonance frequencies of each modal shape and the harmonic behavior with different damping factors of these devices are presented. Parameters as actuation forces, displacements, natural frequencies and specific displacement corresponding to each modal shape

*Corresponding author: E-mail: tecpoyotl@uaem.mx;

in all devices, are also considered in the analysis.

The simulation results show the modal shapes of all analyzed devices, determining their respective modal frequencies and harmonic response. Damping factors of 1% to 10% were employed. The phase angle ($\pm 90^\circ$ to $\pm 105^\circ$) and attenuation levels due to damping were also obtained.

Keywords: Chevron actuator; modal analysis; resonance frequency; cantilever; ansys workbench; harmonic response; mem actuators; microgripper.

1. INTRODUCTION

Nowadays, design engineers and many enterprises are interested in evaluate the mode shapes in which a device or structural element behaves in accordance to dynamics input caused by vibrations [1]. This development is an important step in the manufacture of dynamic or static devices. In Micro-Electro-Mechanical Systems (MEMS) technology, there is an important interest in the characterization of these devices using dynamic analysis, which is a technique to determine the dynamic behavior of a structure or component, involving the time, the inertia and possibly damping of the structure [2]. Their dynamic behavior can be calculated with the dynamic analysis, deformations or displacements, actuation forces, modal shapes, natural frequencies, harmonic responses, spectrum responses, random vibrations and transient analyses [3-8]. A powerful tool that facilitates the analysis and calculation, using finite element method (FEM), or finite element analysis (FEA), is based on the idea of building a complicated object with simple blocks, or, dividing a complicated object into small and manageable pieces. The application of this simple idea can be found in daily life as well as in engineering [9-14].

Mechanical sensor produce a mechanical response, a bending or deflection, when temperature changes are given [15,16].

A *cantilever* is fixed at one end, while the other one is free to move when it experiences some stress (Fig. 1a). A Microcantilever is a device that can be used as physical, chemical or biological sensor by detecting the changes in cantilever bending or vibrational frequency. These microcantilevers produce a deflection at the free end when force is applied. As their dimensions are in micrometers and the amount of applied stress is slight, the deflection will be also in micrometers. This device is frequently used in complexes systems [7-10,17,18].

Chevron-type electrothermal V-actuators use an array of silicon beams facing each other in pairs to generate one directional shuttle. Heating of beam-pairs causes them to expand and ultimately buckle. The beams are designed with a pre-bend angle, so buckling has a tendency to move in-plane (parallel to the substrate) as depicted in Fig. 1b. These actuators typically exhibit forces ranging from just tenths to hundreds of μN . Buckle-beam arrays can develop forces in the order of mN. These devices incorporate the benefits of a chevron actuator in terms of high output force, low operating voltages, sub-micrometer resolution in shuttle positioning, linear movement without deformation of the shuttle, etc. [2,5,10,19].

Manipulation of microparticles can be done using several physical principles and methods. For manipulation of a microstructure, specific ambient conditions are considered, such as in liquid; suction, cryogenic, electrostatic, and friction are the most often considered methods. In recent years, *microgrippers* have been widely studied due to their application areas, such as advanced microassembly, micromanipulation, microrobotics, minimally invasive and living cell surgery. Microgrippers are fabricated using integrated circuits (IC) or IC compatible technology, electrostatic, piezoelectric or electrothermal actuation [3,11,12].

This paper is organized as follows: Section 2 describes the MEM structures under analysis. In the same section, the used modules of Ansys Workbench are described. Physical and mechanical properties of silicon are also given. In section 3, the equations used for simulation of modal and harmonic response analyses are presented. Section four gives the simulation results of each considered device. Finally, in section 5, some concluded remarks are given.

2. METODOLOGY

In the implementation of structures, Professional Autodesk Inventor 2014 is used. The finite element analysis is considered by specific

Ansys-Workbench modules [5] such as: Geometry, Steady-State Thermal, Static Structural, Modal and Harmonic Response. In

Fig. 2, the schematic sequence of analysis process is described.

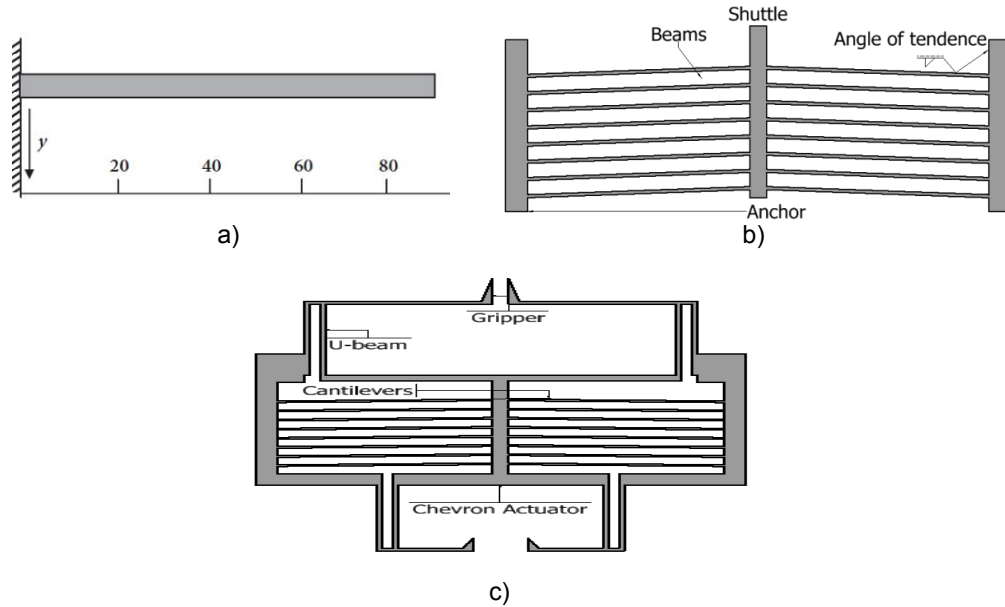


Fig. 1a) Cantilever, b) V-actuator and c) Microgripper

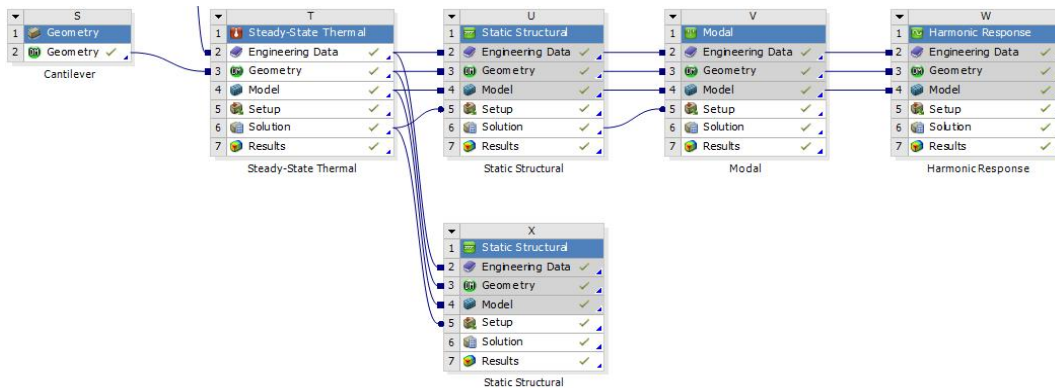


Fig. 2. Schematic project of analysis implemented in Ansys-Workbench

Temperature boundary conditions of MEM devices shown in Fig. 1 are considered:

- For the cantilever (Fig. 1a), the fixed end is fed using a thermal source at 100°C. The free end of beam has room temperature (22°C), as it was realized in [20].
- The V-actuator is formed on the base of an array of symmetric cantilevers, [5,7,19-21], Fig. 1b. In order to increase actuation force and displacements. 8 symmetric beams with 0.9° inclination angle were used. Its

anchor is fixed at 100°C and the shuttle has fixed at room temperature (22°C).

- On the base of V-actuator a microgripper is proposed for specific applications, (Fig. 1c). Its boundary conditions are: The anchor and inferior part are fixed at 100°C, the free gripper at room temperature (22°C). Only upper gripper is analyzed.

These devices were simulated under the mentioned physical and mechanical properties give in Table 1, in order to compare their behavior.

Table 1. Physical and mechanical properties of silicon [6,7]

Properties of silicon	Value
Density [kg/m ³]	2330
Thermal expansion coefficient [1/C]	2.5e-6
Room temperature [°C]	22
Thermal energy source [°C]	100
Young's modulus [Pa]	1.301e11
Poisson's ratio	0.22
Thermal conductivity [W/(m °C)]	148

The analysis process in the Schematic Project of Ansys-Workbench, sequence was carried out as follows:

- At first, geometry is imported from Inventor to Project Schematic.
- Later, in the Steady-State Thermal module, materials and temperatures (power supply and room temperature) are determined and applied.
- In the Static Structural module, the temperature distribution and effects of the structural deformations (total displacement) are evaluated.
- With this deformation value, the actuation force analysis is also realized using the Static Structural module. These parameters allow obtaining the modal shapes and frequency responses of each mode, by means of Modal module and Harmonic response, respectively. Six modals forms were calculated, which will be presented in section 4 (as it is described in [22-25]).
- Finally, with constant values of damping factor in the range 1% to 10% of the total response of the analyzed devices (as it is realized in [26]) and with Harmonic Response module the central frequency and phase angle of all devices is obtained.

In Table 2 the dimensions of cantilever are shown.

3. MATHEMATICAL DESCRIPTION (MODAL AND HARMONIC RESPONSE)

3.1 Description of Modal Analysis

A modal analysis is a technique used to determine the vibration characteristics of structures [26-33]. The vibration of bodies are divided in three main categories: free, forced, and self-excited vibrations.

Table 2. Dimensions of devices

Parameters	[m]
Cantilever	
Weight (W)	3e-6
Thickness (t)	2e-6
Large (L)	200e-6
V-Actuator	
Shuttle length (L)	200e-6
Shuttle width (W)	15e-6
Shuttle thickness (t)	2e-6
Anchor length (L)	200e-6
Anchor width (W)	20e-6
Anchor thickness (t)	2e-6
Microgripper	
U-beam width (W)	10e-6
U-beam length (L)	
U beam separation	325e-6
Gripper ends separation	15e-6

3.1.1 Free vibration

Free vibration occurs in the absence of a long term, external excitation force. It is the result of some initial conditions imposed on the system, such as a displacement from the system's equilibrium position, for example. Free vibration produces motion in one or more of the system's natural frequencies and, because all physical structures exhibit some form of damping (or energy dissipation), it is seen as a decaying oscillation with a relatively short duration [1,13,24].

3.1.2 Forced vibration

Forced vibration takes place when a continuous, external periodic excitation produces a response with the same frequency as the forcing function (after the decay of initial transients). While free vibration is often represented in the time-domain, forced vibration is typically analyzed in the frequency and enables the convenient identification of natural frequencies. A typical source of forced vibration in mechanical systems is rotating imbalance. Large vibrations occur when the forcing frequency, ω , is near to the system natural frequency, ω_n [1,2,16,24,34].

3.1.3 Self-excited vibration

In self-excited vibration, a steady input force is present, as in the case of forced vibration. However, this input is modulated into vibration at one of the system's natural frequencies, as with free vibration. The physical mechanism, that provide this modulation, are varied. Common

examples of self-excited vibration include playing a violin, flutter in airplane wings, and chatter in machining [16,24].

With modal analysis in Ansys-Workbench Software, the characteristic vibrations can be calculated: Natural frequencies and Modal shapes.

3.1.3.1 Mathematical modeling of modal analysis

This analysis considered the motion equation for an undamped linear (with constant stiffness and mass) system, which is used for natural frequency and modal shape determination. The equations were taken from [26], and complemented with some values as follows.

Where:

$$[M]\{\ddot{u}\} + [C]\{\dot{u}\} + [K]\{u\} = \{F\} \quad \text{Eq. 1}$$

- [K] Structural stiffness matrix
- [M] Structural mass matrix
- { \ddot{u} } Nodal acceleration vector
- { \dot{u} } Nodal velocity vector or natural modes
- [C] Structural damping matrix

With:

$$[K] = \sum_{e=1}^N [K^e], \quad [M] = \sum_{e=1}^N [m^e], \\ y\{F\} = \sum_{e=1}^N [f^e]$$

the global stiffness, mass and force matrices, respectively [35]. Note that the global mass matrix is assembled in the same manner as the global stiffness matrix. Equation 1 represents a set matrix equations discretized with respect to space. Discretization in time is also necessary to solve it [36].

Natural frequencies are determined by solving Eq. 1 in the absence of a forcing function F (t). Therefore, the matrix equation with F = 0 and C = 0 is solved:

$$[M]\{\ddot{u}\} + [K]\{u\} = \{0\} \quad \text{Eq. 2}$$

Assuming harmonic motion:

$$\begin{aligned} \{u\} &= \{\phi\}_i \sin(\omega_i t + \theta_i) \\ \{\dot{u}\} &= \omega_i \{\phi\}_i \cos(\omega_i t + \theta_i) \\ \{\ddot{u}\} &= -\omega_i^2 \{\phi\}_i \sin(\omega_i t + \theta_i) \end{aligned} \quad \text{Eq. 3}$$

Where:

- ω_i : Circular frequency of eigenvalue
- { ϕ }_i: Circular frequency of eigenvector

t: Harmonic response time

Substituting the values given in equation 2 in equation 1 and simplifying, with phase = ($\omega_i t + \theta_i$) = 90°, the followed equation can be obtained:

$$\begin{aligned} [M]\{\ddot{u}\} + [K]\{u\} &= \\ -\omega_i^2 [M]\{\phi\}_i \sin(\omega_i t + \theta_i) + [K]\{\phi\}_i \sin(\omega_i t + \theta_i) &= \text{Eq. 4} \\ (-\omega_i^2 [M] + [K])\{\phi\}_i &= \end{aligned}$$

The last equality of equation 3 is satisfied if { ϕ }_i = 0 (trivial solution, implies no vibration) or if:

$$\det([K] - \omega_i^2 [M]) = \{0\} \quad \text{Eq. 5}$$

This is an eigenvalue problem which may be solved for up to n eigenvalues, ω_i^2 , and n eigenvectors, { ϕ }_i, where n is the number of Degrees of Freedom (DoF) or elements that conform a structure in the solver. Note that equation 4, has one more unknown quantity than equations number. Therefore, an additional equation is needed to find a solution. The additional equation is provided by modal shape normalization.

Modal shapes can be normalized either to the mass matrix or to unity, where the largest component of the vector { ϕ }_i, is set to 1, producing the following equation:

$$\{\phi\}_i^T [M] \{\phi\}_i = 1 \quad \text{Eq. 6}$$

Which can be solved on the base of eq. 1-4, using one of two solvers available in workbench mechanical software.

In most cases, the program-controlled option selects the optimal solver automatically.

3.2 Harmonic Response Analysis

This technique is used to determine the steady state response of a structure to harmonic loads of known frequency. This analysis solves the time dependent equations of motion for linear structures subject to steady state vibration [26], with:

Input

- Harmonic loads (forces, pressures, and imposed displacements) of known magnitude and frequency.

- Multiple loads may be at the same frequency. Forces and displacements can be in phase or out of phase. Body loads can only be specified with a phase angle of zero.

- Acceleration, modals and moment loads are assumed to be real (in phase) only.

3.2.2 Mathematical modeling of harmonic response analysis

Output

- Harmonic displacements at each DoF, usually out of phase with the applied loads.
- Other derived quantities, such as stresses and strains.

General equation of motion for a structural system is considered [26]:

$$[M]\{\ddot{u}\} + [C]\{\dot{u}\} + [K]\{u\} = \{F\} \quad \text{Eq. 7}$$

3.2.1 Restrictions of harmonic response analysis [26]

Restrictions

- The entire structure has constant or frequency-dependent stiffness, damping and mass effects.
- All loads and displacements vary sinusoidal, at the same known frequency (although not necessarily in phase)

Where:

- [C] Structural damping matrix
- {u} Nodal displacement vector
- {F} Applied loads vector

Assuming [F] and {u} are harmonic with frequency Ω :

$$\begin{aligned} \{F\} &= \{F_{\max} e^{i\psi}\} e^{i\Omega t} & \{u\} &= \{u_{\max} e^{i\psi}\} e^{i\Omega t} \\ &= \{F_{\max} (\cos \psi + i \sin \psi)\} e^{i\Omega t} & &= \{u_{\max} (\cos \psi + i \sin \psi)\} e^{i\Omega t} \\ &= (\{F_1\} + i\{F_2\}) e^{i\Omega t} & &= (\{u_1\} + i\{u_2\}) e^{i\Omega t} \end{aligned} \quad \text{Eq. 8}$$

Note: The symbols Ω and ω differentiate the input from the output:
 Ω : input circular frequency
 ω : output circular frequency

Taking two time derivatives of u:

$$\begin{aligned} \{u\} &= (\{u_1\} + i\{u_2\}) e^{i\Omega t} \\ \{\dot{u}\} &= i\Omega (\{u_1\} + i\{u_2\}) e^{i\Omega t} \\ \{\ddot{u}\} &= -\Omega^2 (\{u_1\} + i\{u_2\}) e^{i\Omega t} \end{aligned} \quad \text{Eq. 9}$$

Substituting equation 8 and 9, in equation 6, and simplifying:

$$\begin{aligned} [M]\{\ddot{u}\} + [C]\{\dot{u}\} + [K]\{u\} &= \{F\} \\ -\Omega^2 [M](\{u_1\} + i\{u_2\}) e^{i\Omega t} &+ i\Omega [C](\{u_1\} + i\{u_2\}) e^{i\Omega t} \\ + [K](\{u_1\} + i\{u_2\}) e^{i\Omega t} &= (\{F_1\} + i\{F_2\}) e^{i\Omega t} \end{aligned} \quad \text{Eq. 10}$$

$$(-\Omega^2 [M] + i\Omega [C] + [K])(\{u_1\} + i\{u_2\}) = (\{F_1\} + i\{F_2\})$$

Equation 10 can then be solved using one of the following two methods:

The full method solves the system of simultaneous equations directly using a static solver designed for complete arithmetic solution:

Where:

- C denotes a complex matrix or vector

$$\begin{aligned} \overbrace{(-\Omega^2[M] + i\Omega[C] + [K])}^{[K_c]} \overbrace{(\{u_1\} + i\{u_2\})}^{\{u_c\}} &= \overbrace{(\{F_1\} + i\{F_2\})}^{\{F_c\}} \\ [K_c]\{u_c\} &= \{F_c\} \end{aligned} \tag{Eq. 11}$$

Or the mode-superposition method, which expresses the displacements as a linear combination of modal shapes.

$$\begin{aligned} (-\Omega^2[M] + i\Omega[C] + [K])\{u_1\} + i\{u_2\} &= (\{F_1\} + i\{F_2\}) \\ &\vdots \\ (-\Omega^2 + i2\omega_j\Omega\zeta_j + \omega_j^2)v_{jc} &= f_{jc} \end{aligned} \tag{Eq. 12}$$

4. SIMULATION RESULTS

All results were obtained using Ansys Workbench, on the base of two mathematical models presented in section 3. The boundary mechanical and thermal conditions, geometrical and physical data and restrictions for each device were provided, for each corresponding simulation.

The displacement, actuation force, modal frequencies, and harmonic response for cantilever, V-shape actuator and microgripper are summarized in Tables 3-5.

Modal forms and Harmonic Response are given for each device in Tables 6-8.

Table 3. Results of microcantilever

Boundaries conditions	Results	Ansys workbench module
• Fixed beam end	Displacement on Y axis = 20.95 nm	Steady-state thermal
• Fixed end fed with a temperature source of 100°C	Actuation force = 1.5949 nN	Static structural
• Free end at room temperature (22°C)		
Restrictions	Results	Ansys workbench module
	6 modal shapes	
	Mode	Frequency
		Deformation (nm)
• Constant mass	1	90.589 kHz
• Constant stiffness	2	264.01 kHz
• Without damping	3	567.19 kHz
• Free vibration	4	855.24 kHz
	5	1.5857 MHz
	6	1.7833 MHz
		26.18
• Damping factor	Damping factor utilized with 1%, 2%, 4%, 6%, 8% and 10% of total response, as it was developed in [26].	
• Constant displacement	Resonance frequency ~ 5 MHz	
• Constant force	Phase angle ~ 100°	
• Constant frequency	Max. Amplitude with damping factor in 1% ~ 500 nm	
		Modal
		Harmonic response

Table 4. Results of V-shape thermal actuator

Boundaries conditions	Results	Module of Ansys workbench
• Fixed anchors	Displacement on Y axis = 1.22 μm	Steady-state thermal
• Anchors fed with a temperature source of 100°C	Actuation force = 34.9 μN	Static structural
• Shuttle at room temperature (22°C)		
Restrictions	Results	Ansys workbench module
	6 Modal shapes	
	Mode	Frequency kHz
		Deformation (μm)
• Constant mass	1	21.50
• Constant stiffness	2	140.07
• Without damping	3	175.26
• Free vibration	4	228.84
	5	259.06
	6	292.09
• Damping factor	Damping factor utilized with 1%,	
• Constant displacement	2%, 4%, 6%, 8% and 10% of the	
• Constant force	total response, as it was developed	
• Constant frequency	in [26].	
	Resonance frequency ~ 153 Mhz	
	Phase angle ~ - 90°	
	Max. Amplitude with damping	
	factor in 1% ~ 13.3 μm	

Table 5. Results of microgripper

Boundaries conditions	Results	Module of Ansys workbench
• Fixed anchors	Displacement in Y axis = 0.4407 μm	Steady-state thermal
• Anchors fed with a temperature source of 100°C	Actuation Force = 309 μN	Static structural
• Shuttle at room temperature (22°C)		
Restrictions	Results	Ansys workbench Module
	6 Modal shapes	
	Mode	Frequency (kHz)
		Deformation (μm)
• Constant mass	1	40.068
• Constant stiffness	2	41.158
• Without damping	3	87.642
• Free vibration	4	98.426
	5	107.6
	6	108.9
• Damping factor	Damping factor utilized with 1%, 2%,	
• Constant displacement	4%, 6%, 8% and 10% of total	
• Constant Force	response, as it was developed in	
• Constant frequency	[26].	
	Resonance frequency ~ 100 kHz	
	Phase angle ~ - 105 °	
	Max. Amplitude with damping factor	
	in 1% ~ 0.25 mm	

Table 6. Modal forms and harmonic response of microcantilever

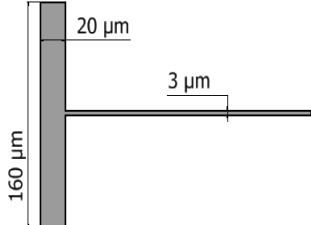
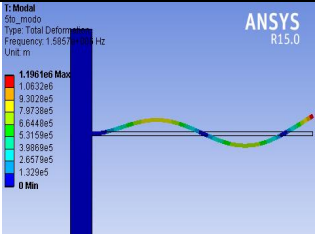
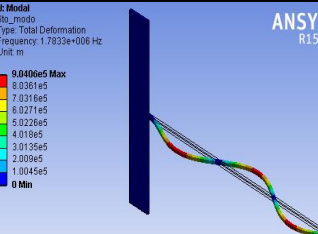
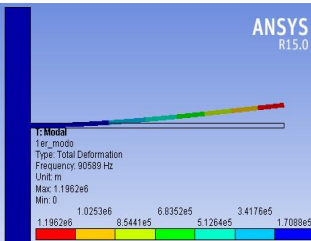
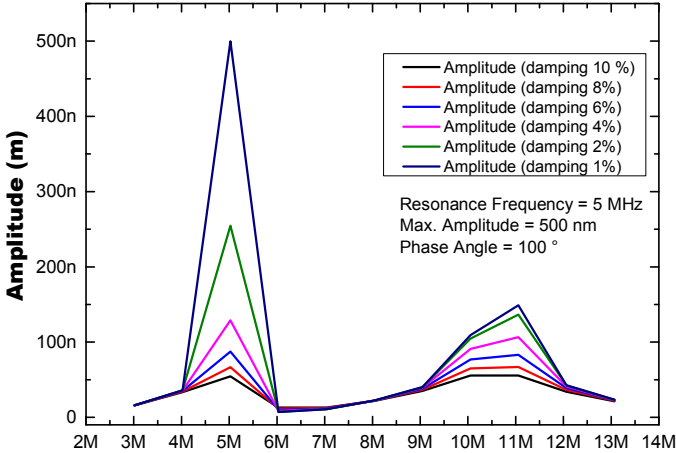
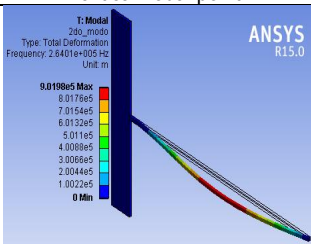
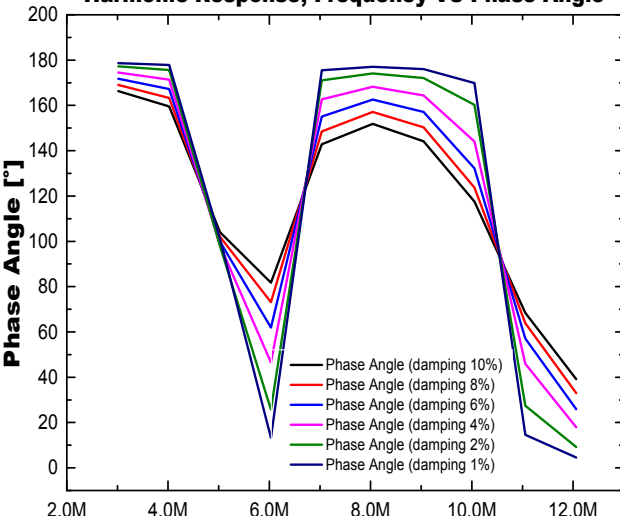
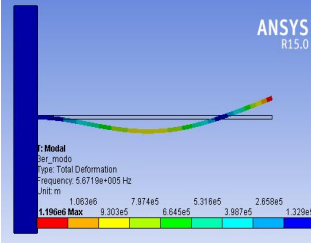
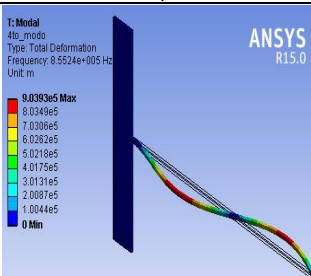
		
<p>Isometric of Microcantilever</p>	<p>5th. Modal form, global vertical bending, three nodal points</p>	<p>6th. Modal form, global horizontal bending, three nodal points</p>
	<div style="text-align: center;"> <p>Harmonic Response, Frequency VS Amplitude</p>  <p>Amplitude (m)</p> <p>Frequency (Hz)</p> <p>Resonance Frequency = 5 MHz Max. Amplitude = 500 nm Phase Angle = 100 °</p> </div>	
<p>1st. Modal form, vertical bending, one critical nodal point</p>	<p>Harmonic Response Scanning (3 to 13) MHz (resonant curve).</p>	
	<div style="text-align: center;"> <p>Harmonic Response, Frequency VS Phase Angle</p>  <p>Phase Angle [°]</p> <p>Frequency (Hz)</p> </div>	
<p>2nd. Modal form, lateral bending, two critical nodal points</p>	<p>Harmonic Response of device with damping factor(1 to 10)%, phase angle 100°</p>	
		
<p>3th. Modal form, torsion, two critical nodal points</p>		
		
<p>4th. Modal form, global horizontal bending, three critical nodal points</p>		

Table 7. Modal forms and harmonic response of device V-shape thermal actuator

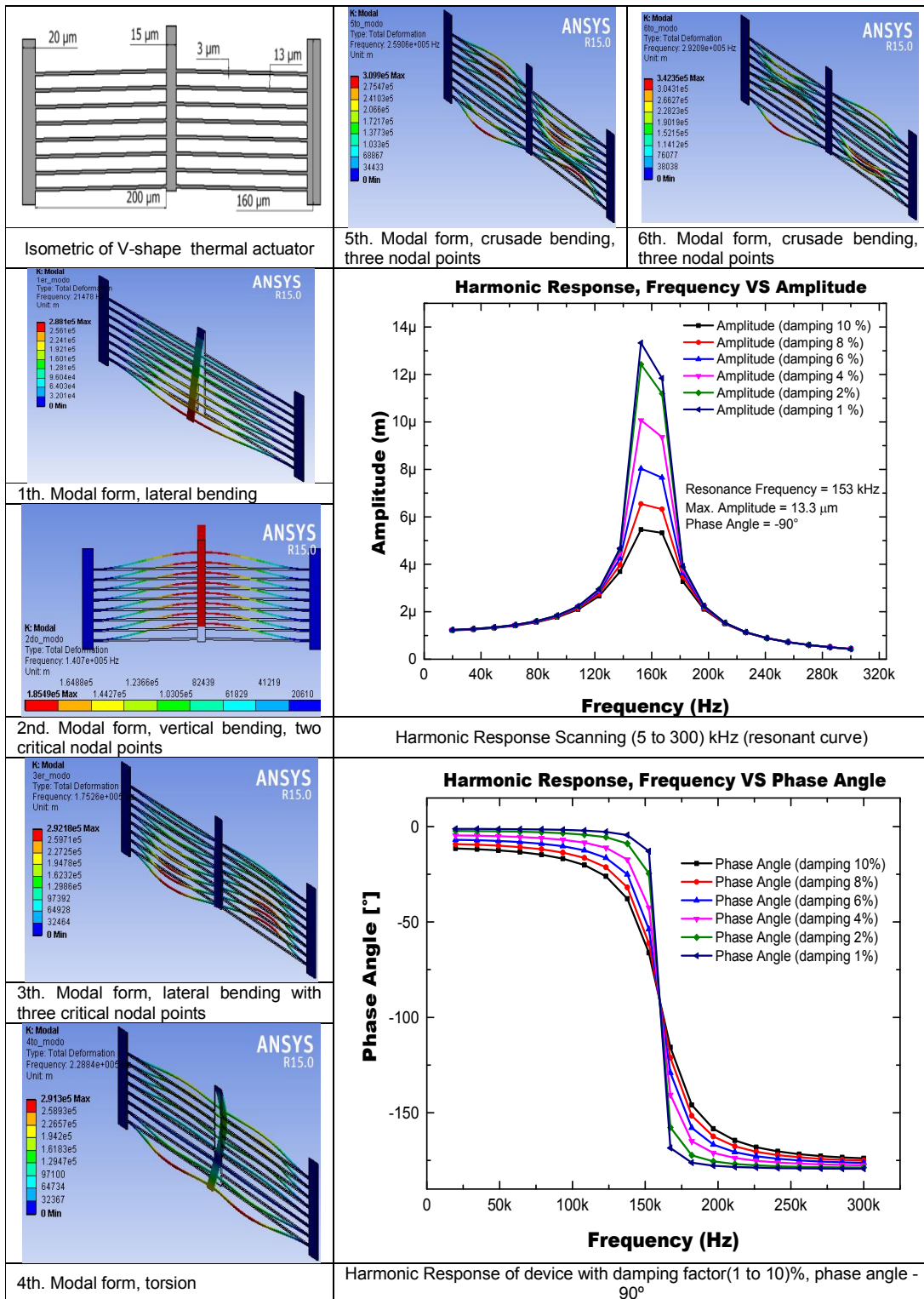


Table 8. Modal forms and harmonic response of microgripper

<p>Isometric of Microgripper</p>	<p>5th. Modal form, partial frontal bending of gripper</p>	<p>6th. Modal form, total frontal bending of gripper</p>
<p>1th. Modal form, total lateral bending of gripper</p>	<p>Harmonic Response Scanning (25 to 250) kHz (resonant curve)</p>	
<p>2nd. Modal form, partial lateral bending of gripper</p>	<p>Harmonic Response of device with damping factor(1 to 10)%, phase angle -105°</p>	
<p>3th. Modal form, central bending of microgripper</p>	<p>4th. Modal form, partial lateral bending</p>	

From Tables 3-5, the following observations were obtained:

- About displacements, the aperture of microgripper is bigger than the case of cantilever, due to the contribution of V-shape actuator. The aperture level is determinant in its possible application, such as microcellular manipulations.
- The actuation force of microgripper is also bigger than the other cases (309 μN). This data can be also of interest for certain applications.
- The conventional use of cantilever corresponds to the first modal form, in this case, given at 90.589 KHz.
- In the case of V-shape actuator, its conventional use corresponds to 2nd modal shape, in this case given at 140 KHz.
- For the microgripper, the knowledge of modal shapes allow us to determine the frequency to operate it. In this case, the appropriate modal shape corresponds to 6th mode, given at 108.9 kHz. The geometry is determinant in the dynamic response of devices.
- Constant damping factors are considered on the total response of each device. It was observed a decrement on the displacements produced by these factors. In real environments, damping factors can be produced as effect of the medium where device is actuating. Each response can be observed in the graphs of harmonic response, frequency versus Amplitude, given in Tables 6-8. In all cases, the bigger amplitude corresponds to 1% of damping factor.
- In addition, this analysis allow us to determine the maximum amplitude or displacement versus frequency.
- About phase angle, in the case of cantilever, V-shape and microgripper, their angles are in the range 100°, -90°, and -105°.
- As a result of simulation, the movement of each structure in each modal shape give us information about the behavior of the total structure.

In the case of the microgripper, it is possible to choose the more adequate frequency avoiding unappropriated aperture. About design, it is possible to add other structural elements in order to improve its performance.

In Tables 6-8, the critical nodal points are clearly observed. In all cases, displacement is inversely proportional to the damping factor.

5. CONCLUSION

In each analyzed device, fundamental natural frequencies and their corresponding modal shapes, using FEA, were determined. Steady-State Thermal, Static Structural, Modal and Harmonic Response modules were used, but for further development it could be necessary include Response Spectrum Analysis, Random Vibration Analysis and Transient Analysis.

Parameters of force and displacement of each device were calculated in order obtain the complete response of the microgripper. In addition, it was demonstrate, by means of FEA that the behavior of these structures with constant damping factor produce a phase angle shift of 100°, -90°, and -105°, for the case of cantilever, V-shape actuator and microgripper, respectively. A decrement on the displacement is also observed, accordingly to the damping factor increasing. The resonance frequency for each device is the same for all considered values of the damping factor.

Information obtained with dynamic analysis, for the case of the microgripper, makes possible to choose the more adequate frequency avoiding unappropriated aperture. About design, it is possible to add other structural elements in order to improve its performance.

The modal shapes analysis allows to understand the performance of the analyzed devices under each characteristic frequency, which determine their performance, and gives us the opportunity to choose the more adequate modal shape to complex systems operation and its use for specific applications of complex systems.

The large actuation force (309 μN) of upper microgripper allows it to be used in applications that needs this range of force and low frequency response (resonance frequency 100 kHz). The rear microgripper performance and its possible applications will be analyzed in future work.

ACKNOWLEDGEMENTS

P. Vargas-Chable and R. Cabello-Ruiz gratefully acknowledge financial support from CONACYT scholarship under grants 484392 and 270210, respectively.

COMPETING INTERESTS

Authors have declared that no competing interests exist.

REFERENCES

1. Luo KJ, Flewitt JA, Peering MS, Fleck AN, Milne IW. Three types of planar structure microspring electro-thermal actuators with insulating beam constrains. *Journal of Micromechanics and Microengineering*. 2005;15:1527-1535.
2. Suen SM, Hsieh CJ, Liu CK, David T, Lin W. Optimal design of the electrothermal V-beam microactuator based on GA for stress concentration analysis. *IMECS Hong Kong*. 2011;11.
3. Greminger Michael A, Serdar Sezen A, Nelson Bradley J. A four of freedom MEMS Microgripper with Novel Bi-directional Thermal Actuators. *IEEE/RSJ, International Conference on Intelligent Robots and Systems*. 2005;1166-1171.
4. Nima Mahmoodi Seyed, Jalili Nader, Daqap F. Modeling nonlinear dynamics, and identification of a piezoelectrically actuated microcantilever sensor. *IEEE/ASME Transactions on Mechanics*. 2008;3(1):58-65.
5. Kumar Goel Anuj, Sinha PH, Gupta Dushyant. Analytical modeling and Simulation of MEMS microstructure-microcantilever using FEM. *International Journal of Exploring Emerging Trends in Engineering (IJEETE)*. 2014;1(1):21-24.
6. Mounika Reddy V, Sunil Kumar GV. Design and analysis of microcantilevers with various shapes using comsol multiphysics software. *International Journal of Emerging Technology and Advanced Engineering*. ISSN 2250-2459. 2013;3(3).
7. Murali Krishna Ghatkesar, Viola Barwich, Thomas Braun, Jean-Pierre Ramseyer, Christoph Gerber, Martin Hegner, Hans Peter Lang, Ute Drechsler, Michel Despont. Higher modes of vibration increase mass sensitivity in nanomechanical microcantilevers; 2007. IOP Publishing.
8. Hans Peter Lang, Martin Hegner, Christoph Gerber. *Springer handbook of Nanotechnology: Nanomechanical Cantilever Array Sensors*, MEMS/NEMS and BioMEMS/NEMS, Springer. 2010;427-452.
9. Zurn S, Hsieh M, Smith G, Markus D, Zang M, Hughes G, Nam Y, Arick M, Polla D. Fabrication and structural characterization of a resonant frequency PZT microcantilever. *Institute of Physics Publishing, Smart Materials and Structures*; 2000.
10. Hernández J. Ezequiel, Valenzuela Víctor M, Del Real Jesús M, Mireles Jr. José. Diseño, Simulación, Fabricación y Comparación Experimental de un Micro-Dinamómetro MEMS para la Medición De Fuerza de un Actuador Térmico. *Congr. Int. Ing. Electrón. Mem. Electro*. 2013;35: 226-231. Chihuahua, Chih. México. Spain.
11. Yasser H. Anis, William L. Cleghorn, James K. Mills. Modal analysis of microgrippers used in assembly of MEMS devices. Department of Mechanical and Industrial Engineering, University of Toronto, Proceedings of the International Conference on MEMS, NANO and Smart Systems (ICMENS'05), IEEE Computer Society; 2005.
12. Chu Duc Trinh. Thesis Sensing microgripper for microparticles handling. ISBN: 978-90-8559-158-0, by Optima Grafische, Delft University of Technology. Book; 2007.
13. Chaudhary Monika, Gupta Amita. Microcantilever-based Sensors, Solid State Physics Laboratory, Defence Science Journal. 2009;59(6):634-641. DESIDOC.
14. Aya B. Hugo, Cano M. Ricardo, Zhevandrov B. Petr. Non-Uniform Euler-Bernoulli beams natural frequencies. *Ingeniería e Investigación*. 2011;31(1):7-15.
15. Sandeep Arya, Saleem Khan, Parveen Lehana. Analytic model of microcantilevers as low frequency generator. *Hindawi Publishing Corporation Modelling and Simulation in Engineering*. 2014;7. Article ID 897315.
16. Thiruvengatanathan Pradyumna, Yan Jize, Seshia Ashwin A. Manipulating vibration energy confinement in electrically coupled microelectromechanical resonator array. *Journal of Microelectromechanical Systems*. 2011;1:157-164.
17. Gil M, Manzaneque T, Hernando-García J, Ababneh A, Seidel H, Sanchez Rojas JL, Selective modal excitation in coupled piezoelectric microcantilevers. *Microsyst. Technol*. 2012;18:917-924.
18. Lobontiu Nicolae, Garcia Ephraim. Two microcantilever design: Lumped-parameter

- model for static and Modal analysis. Journal of Microelectromechanical Systems. 2004;13(1):41-50.
19. Chiorean Radu, Dudescu Cristian, Pustan Marius, Hardau Mihail. Deflection determination of V-beam thermal sensors using Digital Image Correlation. Technical University of Cluj-Napoca, B-dul. Muncii 103-105, 400641, Cluj-Napoca, Romania.
 20. Zhu Yong, Corigliano Alberto, Espinosa D. Horacio. A thermal actuator for nanoscale *In situ* microscopy testing: Design and characterization. Journal of Micromechanics and Microengineering, Institute of Physics Publishing. 2006;242-253.
 21. Varona J, Tecpoyotl-Torres M, Hamui A. Anas. Design of MEMS vertical-horizontal chevron thermal actuators. Sensors and actuators A: Physical, pp. 127-130.
 22. Abarca-Jiménez GS, Reyes-Barranca MA, Mendoza-Acevedo S., Munguía-Cervantes JE, Alemán-Arce MA. Modal analysis of a structure used as a capacitive MEMS accelerometer sensor. 11th International Conference on Electrical Engineering, Computing Science and Automatic Control (CCE); 2014.
 23. Brouwer DM, De Jong BR, De MJ, Jansen HV, Van Dijk J, Krijnen GJM, Soemers HMJR. MEMS-based clamb with a passive hold function for precision position retaining of micro-manipulators. IOP publishing. 2009;19:20.
 24. Peter Kohnke. ANSYS Theory Reference, Release 5.6, 001242, Eleventh Edition. SAS IP, Inc; 1999.
 25. Liu Yijun. Lecture notes: Introduction to the Finite Element Method. CAE Research Laboratory, Mechanical Engineering Department, University of Cincinnati; 2003.
 26. Ansys, inc. Proprietary, ANSYS Mechanical, Dynamics; 2009, all rights reserved.
 27. Franck Gerardo, Gennaro Sergio, Lonardi Bruno, Eichhorn José y Bruno Alejandro. Análisis Dinámico de un Chasis de Semirremolque de Servicio Pesado. Asociación Argentina de Mecánica Computacional. 2009;28:503-517. Spain.
 28. Sierzant Lueke Jonathan. Thesis a MEMS-based Fixed-Fixed Folded Spring Piezoelectric Energy Harvester. Department of Mechanical Engineering, Spring; 2014. Thesis.
 29. Schmitz L, Scott Smith K. Machining Dynamics”, book, Frequency Response to Improved Productivity, Springer. 2009;7-54.
 30. Nakasone Y, Yoshimoto S, Stolarski TA. Engineering analysis with ansys software. book, Elsevier. 2008;143-211.
 31. Budynas Richard GY, Nisbett J. Keith, Diseño en Ingeniería Mecánica de Shigley. Octava edición, Mc Graw Hill. 2008;933-951.
 32. Ostasevicius Vytautas, Dauksevicius Rolanas. Microsystems dynamics. Intelligent Systems, Control and Automatization: Science and Engineering, Springer. 2011;44:11-51. Listo.
 33. García Pascual Luis. Aplicación del análisis modal a un problema sencillo de vibraciones torsionales. Anales de mecánica y electricidad, Universidad Pontificia, curso 2001-2002.
 34. Peter Kohnke. ANSYS Theory Reference, Release 5.6”, 001242, Eleventh Edition. SAS IP, Inc; 1999.
 35. Daryl L. Logan. A first course in the finite element method. Fourth edition, Thomson, University of Wisconsin-Platteville. 2007; 16.
- Reference to Web-resource or Electronic Articles**
36. Huei-Huang Lee. Part and assembly modeling with ANSYS design modeler 14”, Department of Engineering Science National, University Tainan, Taiwan. Available:[http://myweb.ncku.edu.tw/~hhlee/Myweb at NCKU/ADM14.html.listo](http://myweb.ncku.edu.tw/~hhlee/Myweb%20at%20NCKU/ADM14.html.listo)

© 2015 Torres et al.; This is an Open Access article distributed under the terms of the Creative Commons Attribution License (<http://creativecommons.org/licenses/by/4.0>), which permits unrestricted use, distribution, and reproduction in any medium, provided the original work is properly cited.

Peer-review history:
 The peer review history for this paper can be accessed here:
<http://www.sciencedomain.org/review-history.php?iid=1139&id=5&aid=9424>